Transient simulation of the hydrogen-assisted self-ignition of fuel-lean propane-air mixtures in platinum-coated micro-combustors using reduced-order kinetics

JUNJIE CHEN*, DEGUANG XU
School of Mechanical and Power Engineering
Henan Polytechnic University
2000 Century Avenue, Jiaozuo
P.R.CHINA
concjj@163.com; concjj@yahoo.com

Abstract: - Transient simulation of the hydrogen-assisted self-ignition of propane-air mixtures under ambient condition were carried out in platinum-coated micro-combustors, using a two-dimensional model with reduced-order reaction schemes, heat conduction in the solid walls, convection and surface radiation heat transfer. The self-ignition behavior of the hydrogen-propane mixed fuel is compared for the case of heated feed is analyzed. Simulations indicate that hydrogen can successfully cause self-ignition of propane-air mixtures in catalytic micro-channels with a 0.2 mm gap size, eliminating the need for startup devices. The minimum hydrogen composition for propane self-ignition is found to be in the range of 0.8-2.8 % (on a molar basis), and increases with increasing wall thermal conductivity, and decreasing inlet velocity or propane composition. Higher propane-air ratio results in earlier ignition. The ignition characteristics of hydrogen-assisted propane qualitatively resemble the selectively inlet feed preheating mode. Transient response of the mixed hydrogen-propane fuel reveals sequential ignition of propane followed by hydrogen. Front-end propane ignition is observed in all cases. Low wall thermal conductivities cause earlier ignition of the mixed hydrogen-propane fuel, subsequently resulting in low exit temperatures. The transient-state behavior of this micro-scale system is described, and the startup time and minimization of hydrogen usage are discussed.

Key-Words: - Micro-combustion; Catalytic combustion; Transient combustion modelling; Platinum catalyst; Self-ignition; Reduced-order kinetics

1 Introduction

In order to meet the demand for portable power sources with high energy density, recent experiments have focused on utilizing hydrocarbon fuels as energy sources to replace conventional battery [1-4]. The latter has low volumetric and gravimetric power density, relatively short life cycle and is made of materials that are difficult to recycle. The high specific energy of hydrocarbon fuels (approximately 40 $MJ \cdot kg^{-1}$ versus 0.5 $MJ \cdot kg^{-1}$ for lithium-ion battery) [5, 6] and the ability to recharge a hydrocarbon-fueled power source, by merely adding more fuel, are driving attributes of a future fuel-to-electricity technology.

One approach to extract power is the direct combustion of hydrocarbon fuels in micro-combustors to produce power and/or heat. Efforts to utilize hydrocarbons combustion in micro-scale devices have resulted in designs that are scaled down versions of large-scale power generating devices [7,

8]. However, the requirements for moving parts along with the higher temperatures of self-sustaining homogeneous flame in these micro-scale devices challenge devices capable, such as sealing, insulation, and fabrication, etc. Another alternative approach is to combust the hydrocarbon fuels in micro-reactors, with minimal moving parts resulting in further reduction of system size, to produce heat which can be converted into electrical power using thermoelectric energy conversion modules [9-12]. The increased surface to volume ratio of such micro-scale devices leads to considerable radical quenching and heat losses, resulting in unsustainable homogeneous flame [13-16]. Catalytic combustion in such micro-scale devices is preferred because the surface reaction occurs at much lower temperatures and can be sustained at much leaner fuel-air ratios as compared with homogeneous flame [17, 18], and therefore easing the design constraints of the micro-scale system. Furthermore, fuel ignition occurs at

much lower temperatures, and certain fuels such as hydrogen and methanol have been found to be self-starting and self-sustained at the micro-scale, eliminating the need for startup devices [19, 20].

Hydrogen-air mixtures have been found to be self-igniting over platinum wires and foils under fuel-leaner conditions [19, 21, 22] but fuel-richer mixtures exhibit ignition temperature above room temperature. In addition, catalytic combustion of hydrogen over the noble metal catalysts has low activation energy, resulting in extremely fast reaction. The self-ignition nature of hydrogen-air mixtures in ceramic micro-combustors offers an opportunity to self-ignite hydrocarbon fuels, referred to as hydrogen-assisted ignition [19, 23, 24]. This concept may be a way toward elimination of ignition sources from micro-scale devices, resulting to further reduction of micro-scale system size. In addition, since hydrogen is a main target for fuel cell applications, one can envision storage of small amounts of hydrogen during micro-scale device operation from reforming of hydrocarbons that is subsequently used for startup.

Most of the work in literatures has focused on steady-state behavior, including flame stability [25-29], dynamic instabilities [30], thermal management [31] , interaction of homogeneous and heterogeneous chemistry [32], coupling of exothermic and endothermic reactions [33, 34], nonlinear dynamics [35], and strategies to recycle 'excess enthalpy' [36] via reverse-flow operation [37] or heat recirculation [38]. These studies give a good understanding with respect to the steady-state combustion process. However, they do not provide any information on the timescales of these processes. It is important to explore the transient behavior of the micro-combustor during start-up under ambient condition and changing input conditions.

In the case of propane, where external heating is necessary to ignite propane-air mixtures, and fuel adsorption on platinum is slower [19]. Propane-air mixtures also exhibit auto-thermal behavior, namely, they can be self-sustained. Here, we explore the feasibility of this idea, compute the necessary hydrogen content needed to self-ignite propane-air mixtures, and investigate the synergism of binary fuels. The main objective of the present work is to delineate the transient behavior of hydrocarbon self-ignition in micro-combustors. The present study undertakes the numerical investigation of hydrogen-assisted self-ignition of propane-air mixtures in catalytic micro-combustors under ambient condition.

Transient simulations are performed, which include two-dimensional gas-phase description, heat conduction in the solid wall, convection and surface radiation heat transfer, and reduced-order reaction model, to investigate the start-up processes.

2 Numerical Models and Simulation Approach

2. 1 Model Geometry and Mesh

A schematic of the catalytic micro-combustor is shown in Fig. 1. The micro-combustor is modeled as two parallel plates, infinitely wide plates of gap distance $d = 0.2$ mm apart, length $l = 20.0$ mm, and solid wall thickness $\delta = 0.2$ mm. The adopted 0.2 mm geometrical confinement is typical of either catalytic honeycomb reactors for large-scale power generation [39] or of single-channel micro-reactors for portable power generation [20]. Platinum catalyst is coated on the inner channel surfaces, and its properties are listed in Table 1. FLUENT-KINETICS was used to perform these transient simulations.
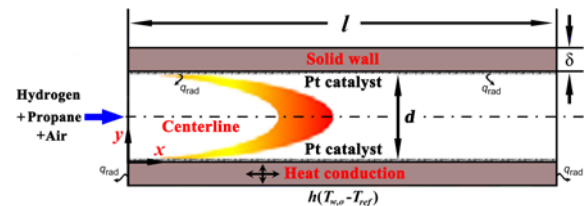
Figure 1. Schematic diagram of the micro-combustor geometry

TABLE 1. The properties of platinum-coated catalyst

Property	Value
catalyst surface site density Γ (mol/cm^2)	2.7×10^{-9}
average pore diameter d_{pore} (m)	2.08×10^{-8}
catalyst porosity ε_{cat}	0.4
catalyst tortuosity τ_{cat}	8.0

2. 2 Chemical Kinetics for Catalytic Combustion of Hydrogen

A reduced-order reaction scheme is used to describe the oxidation of hydrogen over platinum, proposed by Bui et al. [40].

$$-r_{cat,H_2} = \eta A_0 T^{\beta} e^{\frac{-E_{a,H_2}^{ads}}{RT}} C_{H_2} \qquad (1)$$

where effectiveness factor (η), pre-exponential factor (A_0), temperature exponent (β) and activation energy

($E_{a,H2}$) of hydrogen adsorption is 1.0, 1280 cm·K$^{-0.5}$·s^{-1}, 0.5 and 0 kJ·mol^{-1}, respectively. Simulations with this scheme have reproduced measured catalytic ignition temperatures of fuel-lean hydrogen-air mixtures over rhodium and platinum surfaces [41]. A minimum hydrogen-air ratio of homogenous light-off was found at approximately 0.33 [20, 40, 42]. Therefore, homogeneous chemistry of hydrogen was neglected and simulations were restricted for hydrogen-air ratio below 0.2.

2. 3 Chemical Kinetics for Catalytic Combustion of Propane

The reduced-order rate kinetics [40] for the oxidation of propane on platinum is described as follow:

$$r_{cat, C_3H_8} = \frac{k_{C_3H_8}^{ads} C_{s, C_3H_8}}{\left(1 + \sqrt{\frac{k_{O_2}^{ads} C_{s, O_2}}{k_{O_2}^{des}}}\right)^2} \qquad (2)$$

where $r_{cat,C3H8}$, $Cs_{,i}$ and k_i are the surface reaction rate of propane, the concentration of adsorbed species i and the ad-/desorption rate constant of species i, respectively. The latter is determined as follows:

$$k_i^{ads} = \frac{s_0}{\Gamma M_i} \sqrt{\frac{RT}{2\pi T}} \left(\frac{T}{T_{ref}}\right)^{\beta_i^{ads}} e^{\frac{-E_{a,i}^{ads}}{RT}} \qquad (3)$$

$$k_i^{des} = A_0 \left(\frac{T}{T_{ref}}\right)^{\beta_i^{des}} e^{\frac{-E_{a,i}^{des}}{RT}} \qquad (4)$$

where s_0, Γ, M_i and T_{ref} are the sticking coefficient, the surface site density of platinum catalyst, the molecular weight of species i, and the temperature of reference conditions, respectively. The values of these kinetic parameters are given in Table 2. Activation energy of oxygen desorption depends on the coverage of oxygen radical, given as follow:

TABLE 2. kinetic parameters for the catalytic combustion of lean propane over platinum

	A_0 (s^{-1}) or s_0	β	E_a (kcal·mol^{-1})
C$_3$H$_8$ adsorption	0.06	0.154	4
O$_2$ adsorption	0.0542	0.766	0
O$_2$ desorption	8.41×10^{12}	-0.796	*

* $E_{a,O_2}^{des} = 52.8 - \frac{2.3T}{300} - 32.0 \, \theta_{O_.}$

Surface area factor η = 1.7, the temperature of reference conditions T_{ref} = 300 K.

$$\theta_{O_.} = 1 - \frac{1}{\left(1 + \sqrt{\frac{k_{O_2}^{ads} C_{s,O_2}}{k_{O_2}^{des}}}\right)} \qquad (5)$$

2. 4 Boundary Conditions

Uniform velocity distributions and concentration of the incoming mixture at 300 K were specified at the inlet. The initial temperature of the solid wall is spatially uniform and equal to the incoming mixture temperature. Neumann boundary condition was given at the exit. Non-slip boundary condition was considered for the inner wall. The heat flux between fluid and solid wall is computed using the Fourier's law, and the continuity in temperature links the fluid and solid phases. The discrete ordinates (DO) model was used to consider the effect of interior surface to surface radiation [43]. At exterior surfaces, the total heat-loss rate includes both natural convection and thermal radiation, computed as follow:

$$q = h(T_{w,o} - T_\infty) + \varepsilon\delta(T_{w,o}^4 - T_\infty^4) \qquad (6)$$

where h is the exterior convective heat transfer coefficient with a value of 20 W/m^2·K [44]. $T_{w,o}$ is the outer wall temperature. T_∞ is the ambient temperature of 300K. ε is the emissivity of solid surface, taken to be 0.8. δ is the Stefan-Boltzmann constant.

2. 5 Computation Scheme

The quasisteady-state assumption (QSS) was invoked for the surface and gas-phase chemistry to eliminate the high computational cost of fully transient simulations. Most transient QSS models have employed one dimension description for both the bulk-gas and solid phases. QSS necessitates gas-phase diffusive and convective timescales shorter than the heat conduction timescale in the solid phase, such that the gaseous flow temperature can equilibrate to the wall temperature at any time during the transient start-up process [21]. The integration time step Δt is selected to satisfy the QSS approximation, entailing characteristic chemical reaction, diffusion and convection times shorter than the corresponding heat conduction times in the solid phase. QSS approximation yields excellent agreement with full DNS simulations [21] when such criteria are satisfied. According to the timescale

analysis of Michelon et al. [20], the fixed integration time step Δt = 50.0 ms was selected. This time step is long enough to allow for equilibration of the chemical processes and gas-phase transport and at the same time sufficiently short to resolve the axial solid heat conduction.

Non-uniform meshes were used with more grids distributed in the reaction region near the wall to provide sufficient grid resolution in the computational domain. Grid independence was examined and the final grid density was determined when the centerline profiles of species concentration and temperature do not show obvious difference. Under these criteria, a non-uniform mesh with the distribution of 200×60 grid points in the axial and transverse directions was used. The mass, momentum, energy, species conservation equations and the conjugated heat conduction in solid walls were solved by the computational fluid dynamics (CFD) software, FLUENT-KINETICS. The above conservation equations were solved implicitly with the 2D transient-state double-precision segregated solver using the under-relaxation method. The second-order upwind scheme and the "PISO" algorithm was used to discretize the model and employed to couple the pressure and velocity, respectively. The specific heat, fluid viscosity, and thermal conductivity were calculated using the mass fraction weighted average of species properties. The species specific heat was calculated using the piecewise polynomial fit of temperature. The transient solid energy equation was solved with a second-order accurate, fully implicit scheme and a quadratic backward time discretization [21]. A solution for the coupled solid phase and flow equations was obtained at each time step iteratively: convergence was reached as the solid temperatures at all axial positions do not vary between successive iterations by more than 10^{-5} K.

Gas-phase and surface reaction rates were evaluated with CHEMKIN [45] and Surface-CHEMKIN [46], respectively. Mixture-average diffusion was adopted, and transport properties were calculated from the CHEMKIN transport database [47].

3. Results and Discussions

The micro-combustor initially contains only air, starting at ambient conditions of 300 K. The premixed hydrogen-propane-air mixtures is fed starting at the time t = 0 at the desired inlet velocity and equivalence ratio.

3. 1 Hydrogen Requirement for Propane Self-Ignition

Fig. 2 shows the maximum temperature versus hydrogen mole fraction in hydrogen-assisted mode at an inlet velocity of 10 m/s. In this case, the propane-air ratio is held constant. As the hydrogen concentration increases starting from a zero value, the flow rates of propane and air are reduced, as the hydrogen flow rate increases to maintain the total volumetric flow rate fixed. Simulations indicate that hydrogen can successfully cause self-ignition of propane-air mixtures in catalytic micro-channels with a 0.2 mm gap size, eliminating the need for startup devices. Higher hydrogen compositions result in increased maximum temperature. As the hydrogen composition increases, the maximum temperature increases slowly until approximately the hydrogen mole fraction is approximately 1.7-1.8 %. After a particular hydrogen composition, the heat released by hydrogen oxidation is sufficient to ignite propane and the turning point bifurcation is observed. This bifurcation behavior is consistent with the previous work [19]. The maximum temperature versus inlet temperature in inlet feed preheating mode (without hydrogen addition) are also shown in Fig. 2 for comparison. The temperature of bifurcation point in hydrogen-assisted mode is slightly higher than that in inlet feed preheating mode. In addition, higher equivalence ratio of propane-air mixtures results in earlier ignition.

Fig. 3 shows hydrogen requirement for propane self-ignition of various equivalence ratios at an inlet velocity of 10 m/s. The propane ignition temperature in inlet feed preheating mode is also shown in Fig. 3 for comparison. The minimum hydrogen composition for propane self-ignition is reduced with the increase of propane-air ratio. This behavior is consistent with the experimental observations by Deutschmann et al. [23], who propose that the concentration of hydrogen needed for hydrocarbon ignition decreases as hydrocarbon concentration is increased. This trend in hydrogen-assisted mode is quite similar to that in inlet preheating mode.

Fig. 4 shows hydrogen requirement for propane self-ignition of various wall thermal conductivities. Both wall thermal conductivity and inlet velocity have a significant effect on hydrogen requirement. Higher inlet velocities result in higher wall

temperatures. As a result, hydrogen requirement reduces. Likewise, hydrogen requirement increases with the increase of wall thermal conductivity. This behavior is because the wall hot spots created near the inlet for lower thermal conductivity [20, 31, 38] help the mixtures get ignite with lesser hydrogen. The hydrogen requirement for propane self-ignition varies in the range of 0.8-2.8 % (on a molar basis).
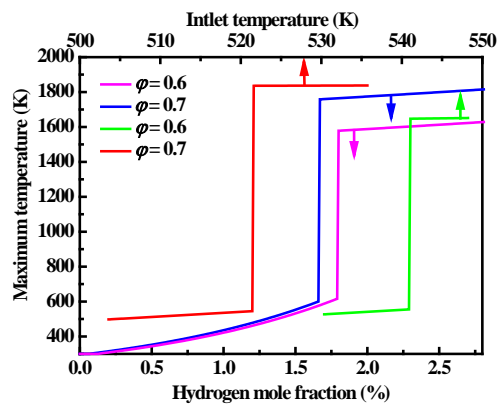
Figure 2. Maximum temperature versus hydrogen mole fraction in hydrogen-assisted mode and inlet temperature in inlet feed preheating mode
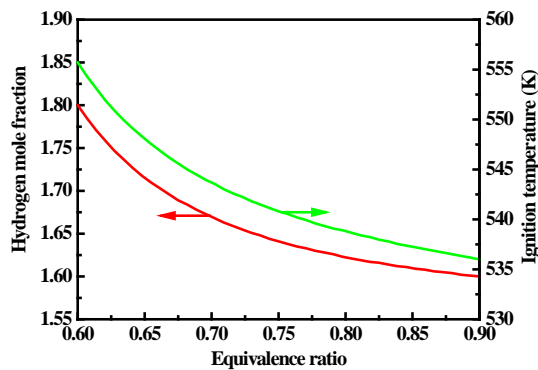
Figure 3. Hydrogen requirement and ignition temperature versus different propane-air equivalence ratios
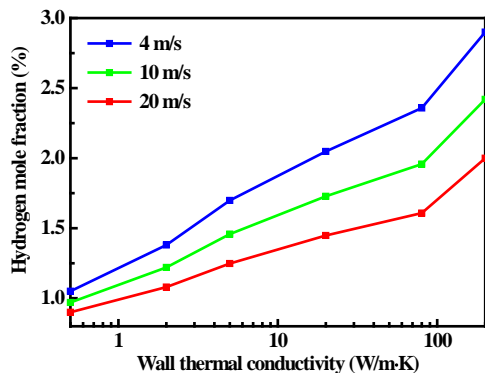
Figure 4. Hydrogen requirement for different inlet velocities and wall thermal conductivities. The parameters used are φ (C$_3$H$_8$) = 0.7 and $h = 20$ W/m^2·K
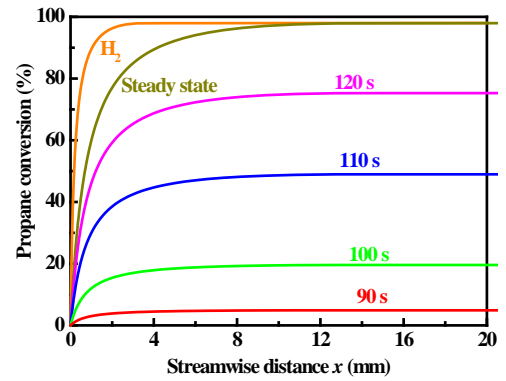
(a) $k_s = 0.5$ W/m·K
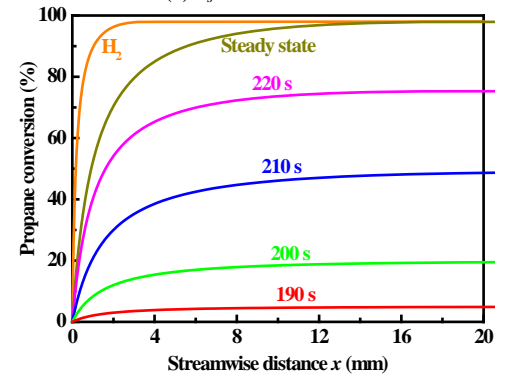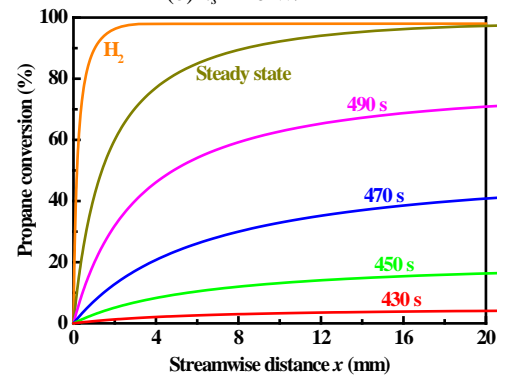
(b) $k_s = 20$ W/m·K

(c) $k_s = 200$ W/m·K

Figure 5. Transient response of propane conversion profiles for various wall thermal conductivities. The parameters used are φ (C$_3$H$_8$) = 0.7, $u_0 = 2$ m/s, and $h = 20$ W/m^2·K

3. 2 Ignition Characteristics and Transient Response

In this case, the propane-air ratio is kept fixed at 0.7, and the amount of hydrogen is 0.05 % (on a molar basis) excess of the minimum amount required for propane self-ignition over platinum in the corresponding case. Transient responses of propane conversion, bulk-gas and interior-wall temperatures versus various wall thermal conductivities at an inlet velocity of 2 m/s are shown in Fig. 5-7, respectively.

(a) $k_s = 0.5$ W/m·K

(b) $k_s = 20$ W/m·K

(c) $k_s = 200$ W/m·K
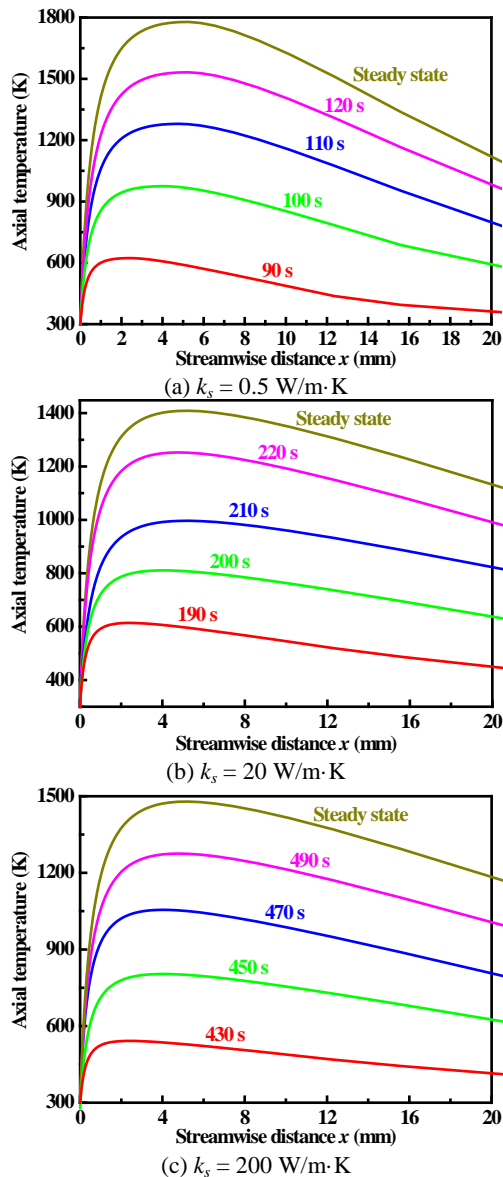
Figure 6. Transient response of bulk gas temperature profiles for various wall thermal conductivities. The parameters used are φ (C_3H_8) = 0.7, u_0 = 2 m/s, and h = 20 W/m²·K

(a) $k_s = 0.5$ W/m·K

(b) $k_s = 20$ W/m·K

(c) $k_s = 200$ W/m·K
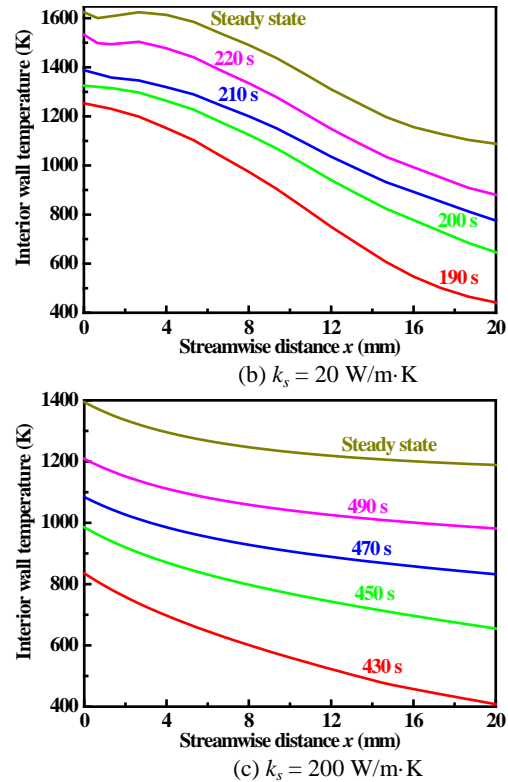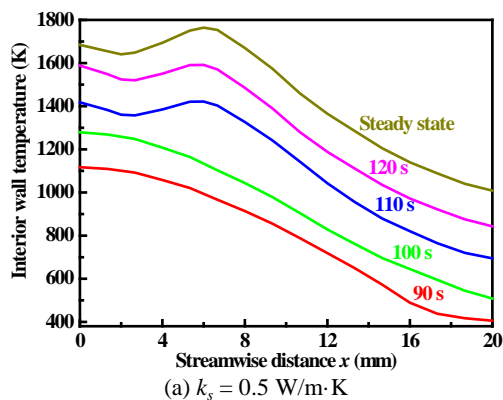
Figure 7. Transient response of interior wall temperature profiles for various wall thermal conductivities. The parameters used are φ (C_3H_8) = 0.7, u_0 = 2 m/s, and h = 20 W/m²·K

Hydrogen ignites in approximately 1.0-2.0 s and directly reaches its steady-state profile, as shown in Fig. 5. Note that the hydrogen conversion profiles change very slightly in most cases. Ignition time t_{ign} is defined as the time taken for catalytic conversion of propane to reach 50.0 % at the exit. As shown in Fig. 6, higher wall thermal conductivity results in the increase in ignition time from 98 s for insulating materials (0.5 W/m·K) to 202 s for materials with moderately wall thermal conductivities (20 W/m·K), and 448 s for materials with higher wall thermal conductivities (200 W/m·K). This trend is caused by the heat localization within the walls with lower thermal conductivities, resulting in hot spot formation and faster ignition. In addition, the front-end ignition is observed in all cases. The bulk-gas and interior wall temperatures reach their steady-state values quickly once propane is ignited. The ignition characteristics in hydrogen-assisted mode qualitatively resemble those in inlet feed preheating mode [26, 48, 49].

Another observation is that the wall temperatures first drop, then increase, and then drop again at steady-state for low conductivity walls (0.5 W/m·K), as observed in Fig. 7. This trend is because hydrogen

combustion region is located significantly upstream as compared with propane. In the region between them, the interior wall temperatures drop slightly as a result of heat losses to the surroundings.

(a) Exit temperature

(b) Propane conversion
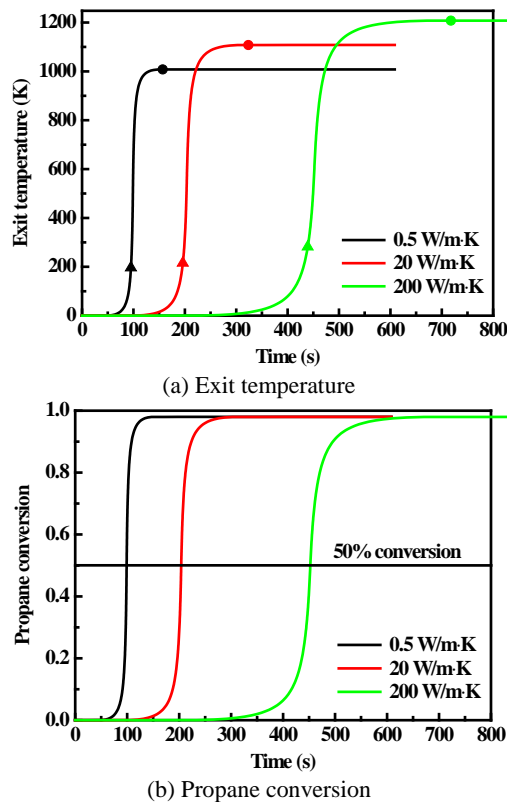
Figure 8. Exit temperature and propane conversion profiles for different wall thermal conductivities. The parameters used are φ (C_3H_8) = 0.7, u_0 = 2 m/s, and h = 20 W/m^2·K. The circles denote the steady state time t_{ss}, and the triangles denote the ignition time t_{ign}.

Fig. 8 shows the temperatures and propane conversions at the exit as a function of the cumulative time for various wall thermal conductivities. The triangles represent the ignition time, at which propane is ignited corresponding to 50.0 % conversion. The circles represent the steady-state time, at which propane combustion taken to reach steady-state. Complete conversion of propane is achieved in all cases. Lower wall thermal conductivities cause earlier ignition of the mixed hydrogen-propane fuel, subsequently resulting in lower exit temperatures.

In general, the premixed fuel-lean hydrogen-propane-air mixtures over platinum can result in self-ignition without the need for an external preheater. The platinum catalyst allows instantaneous ignition of hydrogen, and followed by propane ignition after its ignition temperature is reached. A minimum hydrogen concentration in the range of 0.8-2.8 % (on a molar basis) is needed, and decreases for: lower wall thermal conductivity, higher inlet velocity, and higher propane-air ratio.

4. Conclusions

Transient simulation of the hydrogen-assisted self-ignition of propane-air mixtures were carried out in platinum-coated micro-combustors under ambient condition, using a two-dimensional model with reduced-order reaction schemes, heat conduction in the solid wall, convection and surface radiation heat transfer. It has been shown that hydrogen can successfully cause self-ignition of propane-air mixtures in catalytic micro-combustors with a 0.2 mm gap size, eliminating the need for startup devices. The minimum hydrogen composition for propane self-ignition is found to be in the range of 0.8-2.8 % (on a molar basis), and increases with increasing wall thermal conductivity, and decreasing inlet velocity or propane composition. Higher propane-air ratio results in earlier ignition. The ignition characteristics of hydrogen-assisted propane qualitatively resemble the selectively inlet feed preheating mode. Hydrogen got ignited first, the resulting increase in wall temperature caused subsequent ignition of propane. Front-end propane ignition is observed in all cases. Low wall thermal conductivities cause earlier ignition of the mixed hydrogen-propane fuel, subsequently resulting in low exit temperatures.

References:
[1] C. Deng, W. Yang, J. Zhou, Z. Liu, Y. Wang, and K. Cen. Catalytic combustion of methane, methanol, and ethanol in microscale combustors with Pt/ZSM-5 packed beds. *Fuel*, Vol. 150, pp. 339-346, 2015.
[2] T.A. Wierzbicki, I.C. Lee, and A.K. Gupta. Rh assisted catalytic oxidation of jet fuel surrogates in a meso-scale combustor. *Applied Energy*, Vol. 145, pp. 1-7, 2015.
[3] J. Lu and C.M. Corvalan. Free-surface dynamics of small pores. *Chemical Engineering Science*, Vol. 132, pp. 93-98, 2015.
[4] J.A. Federici, E.D. Wetzel, B.R. Geil, and D.G. Vlachos. Single channel and heat recirculation catalytic microburners: An experimental and

computational fluid dynamics study. *Proceedings of the Combustion Institute*, Vol. 32, No. 2, pp. 3011-3018, 2009.

[5] K. Bijjula and D.G. Vlachos. Catalytic ignition and autothermal combustion of JP-8 and its surrogates over a Pt/γ-Al$_2$O$_3$ catalyst. *Proceedings of the Combustion Institute*, Vol. 33, No. 2, pp. 1801-1807, 2011.

[6] K. Bijjula and D.G. Vlachos. Catalytic ignition and autothermal combustion of JP-8 and its surrogates over a Pt/γ-Al$_2$O$_3$ catalyst. *Proceedings of the Combustion Institute*, Vol. 33, No. 2, pp. 1801-1807, 2011.

[7] S. Akhtar, J.C. Kurnia, T. Shamim. A three-dimensional computational model of H$_2$-air premixed combustion in non-circular micro-channels for a thermo-photovoltaic (TPV) application. *Applied Energy*, Vol. 152, pp. 47-57, 2015.

[8] M.C. Cameretti and R. Tuccillo. Combustion features of a bio-fuelled micro-gas turbine. *Applied Thermal Engineering*, Vol. 89, pp. 280-290, 2015.

[9] P.D. Ronney. Analysis of non-adiabatic heat-recirculating combustors. *Combustion and Flame*, Vol. 135, No. 4, pp. 421-439, 2003.

[10] S. Yadav, P. Yamasani, and S. Kumar. Experimental studies on a micro power generator using thermo-electric modules mounted on a micro-combustor. *Combustion and Flame*, Vol. 99, pp. 1-7, 2015.

[11] A. Rezania and L.A. Rosendahl. A comparison of micro-structured flat-plate and cross-cut heat sinks for thermoelectric generation application. *Energy Conversion and Management*, Vol. 101, pp. 730-737, 2015.

[12] S.E. Hosseini and M.A. Wahid. Investigation of bluff-body micro-flameless combustion. *Energy Conversion and Management*, Vol. 88, pp. 120-128, 2014.

[13] L. Zhang, J. Zhu, Y. Yan, H. Guo, and Z. Yang. Numerical investigation on the combustion characteristics of methane/air in a micro-combustor with a hollow hemispherical bluff body. *Energy Conversion and Management*, Vol. 94, pp. 293-299, 2015.

[14] W. Yang, A. Fan, J. Wan, and W. Liu. Effect of external surface emissivity on flame-splitting limit in a micro cavity-combustor. *Applied Thermal Engineering*, Vol. 83, pp. 8-15, 2015.

[15] J. Lee, S. Jeon, and Y. Kim. Multi-environment

probability density function approach for turbulent CH$_4$/H$_2$ flames under the MILD combustion condition. *Combustion and Flame*, Vol. 162, No. 4, pp. 1464-1476, 2015.

[16] A. Veeraragavan and C.P. Cadou. Flame speed predictions in planar micro/mesoscale combustors with conjugate heat transfer. *Combustion and Flame*, Vol. 158, No. 11, pp. 2178-2187, 2011.

[17] J.A. Badra and A.R. Masri. Catalytic combustion of selected hydrocarbon fuels on platinum: Reactivity and hetero-homogeneous interactions. *Combustion and Flame*, Vol. 159, No. 2, pp. 817-831, 2012.

[18] A. Brambilla, C.E. Frouzakis, J. Mantzaras, A. Tomboulides, S. Kerkemeier, and K. Boulouchos. Detailed transient numerical simulation of H$_2$/air hetero-/homogeneous combustion in platinum-coated channels with conjugate heat transfer. *Combustion and Flame*, Vol. 161, No. 10, pp. 2692-2707, 2014.

[19] D.G. Norton and D.G. Vlachos. Hydrogen assisted self-ignition of propane/air mixtures in catalytic microburners. *Proceedings of the Combustion Institute*, Vol. 30, No. 2, pp. 2473-2480, 2005.

[20] D.G. Norton, E.R. Wetzel, and D.G. Vlachos. Fabrication of single-channel catalytic microburners: Effect of confinement on the oxidation of hydrogen/air mixtures. *Industrial & Engineering Chemistry Research*, Vol. 43, No. 16, pp. 4833-4840, 2004.

[21] N. Michelon, J. Mantzaras, and P. Canu. Transient simulation of the combustion of fuel-lean hydrogen/air mixtures in platinum-coated channels. *Combustion Theory and Modelling, Vol. 19, No. 4, pp. 514-548, 2015.*

[22] *N. Fernandes,* Y.K. Park, and D.G. Vlachos. Transient simulation of the combustion of fuel-lean hydrogen/air mixtures in platinum-coated channels. *Combustion and Flame*, Vol. 118, No. 1-2, pp. 164-178, 1999.

[23] O. Deutschmann, L.I. Maier, U. Riedel, A.H. Stroemman, and R.W. Dibble. Hydrogen assisted catalytic combustion of methane on platinum. *Catalysis Today*, Vol. 59, No. 1-2, pp. 141-150, 2000.

[24] Y. Zhang, J. Zhou, W. Yang, M. Liu, and K. Cen. Effects of hydrogen addition on methane catalytic combustion in a microtube. *International Journal of Hydrogen Energy*, Vol.

32, No. 9, pp. 1286-1293, 2007.

[25] G. Landi, A. Di Benedetto, P.S. Barbato, G. Russo, and V. Di Sarli. Transient behavior of structured $LaMnO_3$ catalyst during methane combustion at high pressure. *Chemical Engineering Science*, Vol. 116, pp. 350-358, 2014.

[26] V. Seshadri and N.S. Kaisare. Ignition strategies for fuel-mixtures in microburners. *Combustion Theory and Modelling*, Vol. 14, No. 1, pp. 23-40, 2010.

[27] J. Mantzaras, R. Bombach, and R. Schaeren. Hetero-/homogeneous combustion of hydrogen/air mixtures over platinum at pressures up to 10 bar. *Proceedings of the Combustion Institute*, Vol. 32, No. 2, pp. 1937-1945, 2009.

[28] P.M. Struk, J.S. T'ien, F.J. Miller, and D.L. Dietrich. Transient numerical modeling of catalytic channels using a quasi-steady gas phase. *Chemical Engineering Science*, Vol. 119, pp. 158-173, 2014.

[29] X. Zheng and J. Mantzaras. An analytical and numerical investigation of hetero-/homogeneous combustion with deficient reactants having larger than unity Lewis numbers. *Combustion and Flame*, Vol. 161, No. 7, pp. 1911-1922, 2014.

[30] G. Pizza, J. Mantzaras, C. Frouzakis, A. Tomboulides, and K. Boulouchos. Suppression of combustion instabilities of premixed hydrogen/air flames in microchannels using heterogeneous reactions. *Proceedings of the Combustion Institute*, Vol. 32, No. 2, pp. 3051-3058, 2009.

[31] D.G. Norton, E.D. Wetzel, and D.G. Vlachos. Thermal management in catalytic microreactors. *Industrial & Engineering Chemistry Research*, Vol. 45, No. 1, pp. 76-84, 2006.

[32] M. Schultze, J. Mantzaras, F. Grygier, and R. Bombach. Hetero-/homogeneous combustion of syngas mixtures over platinum at fuel-rich stoichiometries and pressures up to 14 bar. *Proceedings of the Combustion Institute*, Vol. 35, No. 2, pp. 2223-2231, 2015.

[33] S.R. Deshmukh and D.G. Vlachos. CFD simulations of coupled, countercurrent combustor/reformer microdevices for hydrogen production. *Industrial & Engineering Chemistry Research*, Vol. 44, No. 14, pp. 4982-4992, 2005.

[34] J. Zetterberg, S. Blomberg, J. Gustafson, J. Evertsson, J. Zhou, E.C. Adams, P.-A. Carlsson,

M. Aldén, and E. Lundgren. Spatially and temporally resolved gas distributions around heterogeneous catalysts using infrared planar laser-induced fluorescence. *Nature Communications*, Vol. 6, Article number: 7076, 2015.

[35] A. Brambilla, C.E. Frouzakis, J. Mantzaras, R. Bombach, and K. Boulouchos. Flame dynamics in lean premixed CO/H_2/air combustion in a mesoscale channel. *Combustion and Flame*, Vol. 161, No. 5, pp. 1268-1281, 2014.

[36] G.P. Gauthier, G.M.G. Watson and J.M. Bergthorson. Burning rates and temperatures of flames in excess-enthalpy burners: A numerical study of flame propagation in small heat-recirculating tubes. *Combustion and Flame*, Vol. 161, No. 9, pp. 2348-2360, 2014.

[37] N.S. Kaisare and D.G. Vlachos. Extending the region of stable homogeneous micro-combustion through forced unsteady operation. *Proceedings of the Combustion Institute*, Vol. 31, No. 2, pp. 3293-3300, 2007.

[38] S.K. Som and U. Rana. Wall heat recirculation and exergy preservation in flow through a small tube with thin heat source. *International Communications in Heat and Mass Transfer*, Vol. 64, pp. 1-6, 2015.

[39] R. Carroni, T. Griffin, J. Mantzaras, and M. Reinke. High-pressure experiments and modeling of methane/air catalytic combustion for power generation applications. *Catalysis Today*, Vol. 83, No. 1-4, pp. 157-170, 2003.

[40] P.-A. Bui, E.A. Wilder, D.G. Vlachos, and P.R. Westmoreland. Hierarchical reduced models for catalytic combustion: H_2/Air mixtures near platinum surfaces. *Combustion Science and Technology*, Vol. 129, No. 1-6, pp. 243-275, 1997.

[41] M.S. Mettler, G.D. Stefanidis, and D.G. Vlachos. Enhancing stability in parallel plate microreactor stacks for syngas production. *Chemical Engineering Science*, Vol. 66, No. 6, pp. 1051-1059, 2011.

[42] M. Schultze and J. Mantzaras. Hetero-/homogeneous combustion of hydrogen/air mixtures over platinum: Fuel-lean versus fuel-rich combustion modes. *International Journal of Hydrogen Energy*, Vol. 38, No. 25, pp. 10654-10670, 2013.

[43] C.H. Kuo and P.D. Ronney. Numerical modeling of non-adiabatic heat-recirculating

combustors. *Proceedings of the Combustion Institute*, Vol. 31, No. 2, pp. 3277-3284, 2007.

[44] J. Wan, A. Fan, H. Yao, and W. Liu. Effect of thermal conductivity of solid wall on combustion efficiency of a micro-combustor with cavities. *Energy Conversion and Management*, Vol. 96, pp. 605-612, 2015.

[45] R.J. Kee, F.M. Rupley, E. Meeks, and J.A. Miller. *Chemkin: a Fortran chemical kinetics package for the analysis of gas-phase chemical kinetics*, Report No. SAND96-8216, Technical Report, Sandia National Laboratories, 1996.

[46] M.E. Coltrin, R.J. Kee, F.M. Rupley, and E. Meeks. *Surface Chemkin: a Fortran package for analyzing heterogeneous chemical kinetics at a solid surface/gas-phase interface*, Report No. SAND96-8217, Technical Report, Sandia National Laboratories, 1996.

[47] R.J. Kee, G. Dixon-Lewis, J. Warnatz, M.E. Coltrin, and J.A. Miller. *A Fortran computer code package for the evaluation of gas-phase multicomponent transport properties*, Report No. SAND86-8246, Technical Report, Sandia National Laboratories, 1996.

[48] N.S. Kaisare, G.D. Stefanidis, and D.G. Vlachos. Comparison of ignition strategies for catalytic microburners. *Proceedings of the Combustion Institute*, Vol. 32, No. 2, pp. 3027-3034, 2009.

[49] W. Choi, S. Kwon, and H.D. Shin. Combustion characteristics of hydrogen-air premixed gas in a sub-millimeter scale catalytic combustor. *International Journal of Hydrogen Energy*, Vol. 33, No. 9, pp. 2400-2408, 2008.